# FAILURE ANALYSIS OF A HERRINGBONE GEAR IN 2-HI PINION GEARBOX USED IN HOT STEEL MILL

Somdech Ingkawara[1] and Samroeng Netpu[2]

[1]Lecturer, Department of Industrial Engineering, Faculty of Engineering, Pathumwan Institute of Technology, 833 Rama 1 Road, Wangmai, Pathumwan, Bangkok 10330, Thailand, somdech96@gmail.com

[2]Lecturer, Master of Engineering Program in Engineering Management, Graduate School, Kasem Budit University, 1761 Pattanakarn Road, Suan Luang, Bangkok 10250, Thailand, samroeng.net@kbu.ac.th

## ABSTRACT

This paper describes an investigation of a failure of a herringbone gear in a two high pinion gearbox used in a continuous hot re-rolling steel mill in Thailand. The gear failed prematurely after approximately 10 hours of operation. Standard investigative procedures were employed. It was found that the premature failure of the gear which appeared as a longitudinal crack was due to excessive stress. This excessive stress was the results of improper fit between the key and the keyway. The key was slightly too large for the keyway due to machining errors. It is concluded that poor manufacturing and improper mounting could lead to premature failure of the key components such as gears and could be very costly.

**KEYWORDS:** Failure analysis, Key, Keyway crack, Herringbone gear failure, 2-Hi pinion gearbox

## 1. Introduction

Herringbone gears are key components of gearboxes which transmit power under heavy loads. Such gearboxes are extensively used in steel industry. Failures of gears not only result in replacement cost but also in process downtime. This could have a drastic effect on productivity and, more importantly, late delivery. In this case, for example, the downtime was two weeks and 5,000 metric tons of steels were lost before the failed herringbone gear could be replaced.

Gears fail from a variety of reasons. Gears failure modes include (in decreasing order of frequency) fatigue, impact fracture, wear, stress rupture. Tooth bending fatigue, contact fatigue, and thermal fatigue are among the most common types of fatigue failures in gears [1]. Abrasive wear and adhesive wear are also common modes of gear failures [2]. Tooth surface fatigue occurs when the load is applied on the tooth surface repeatedly, or when the force is applied on the tooth is larger than endurance limit of the material. As the result of the surface fatigue, the material fails and falls off the tooth surface [3]. Gears fail in service like other mechanical elements, for a variety of reasons. Sometimes, rising noise and vibration betray impending gear failure, but often total failure is the only indicator of a problem in a gear train [4]. Several causes of gear tooth failure have been identified in the literature including poor design of gear sets, incorrect assembly or misalignment, overloads, inadvertent stress raisers, subsurface defects in critical areas, and the use of incorrect materials and improper heat treatments [5]. A study on the influence of keyway on stress distribution in thin rimmed pinions showed that not only the hub thickness between the root of the tooth and the keyway has a large influence on the stress but also the position of the gearing in relation to the keyway [6]. An investigation on the effect of rim thickness on gear crack propagation path using FRANC (Fracture analysis code) computer program showed that the crack originated from root fillet surface of gear tooth on the loaded side then propagated inside the gear hub [7]. Stress concentration factor at the root radius where maximum stresses are experienced vary from 1.4-2.5 [8]. An investigation of a herringbone gear failure concluded that the failure was due to excessive stress resulting from keyway misalignment and the crack originated at the root fillet of the keyway [9]. There are three types of errors that can occur when hubs and bores that might lead to failure. The first is incorrect bore diameter. This could result in too much interference which will cause installation problems and hub damage. The second is the bore eccentricity which could lead to the same problems. The third is the misalignment between the bore and the hub [10].

This paper aims at identifying the cause of the herringbone gear failure so that the reoccurrence of similar failure can be avoided or minimized in the future.

## 2. Background

The failed herringbone gear was used in a 2-hi gearbox (2hi-PG) in a hot rolling steel mill in Thailand. The gear failed after approximately 10 hours of operation. Normally, a gearbox has an expected working life of around 40,000-50,000 hours in continuous running conditions [11]. The steel mill produces steel re-bars sized 12-20 mm diameter with a capacity of 30 metric tons per hour.

The 2hi-PG was used in the 1st intermediate stand (7th from the first roughing stand). It was designed for rolling billets with cross-section of 45.0×45.0 $mm^2$ square to cross-section of 72.0×26.4 $mm^2$ oval. The failed gear has 29 teeth and the face width of 390 mm with diametral pitch ($P_d$) 2.25 inch and helix angle 22.50º. The rotation speed of the 2hi-PG was 65 rpm. The 2hi-PG was driven by a reducer gearbox which in turn was driven by a 300 kW AC motor. Relevant layout of the 2hi-PG and the key dimensions are shown in Figure 1.

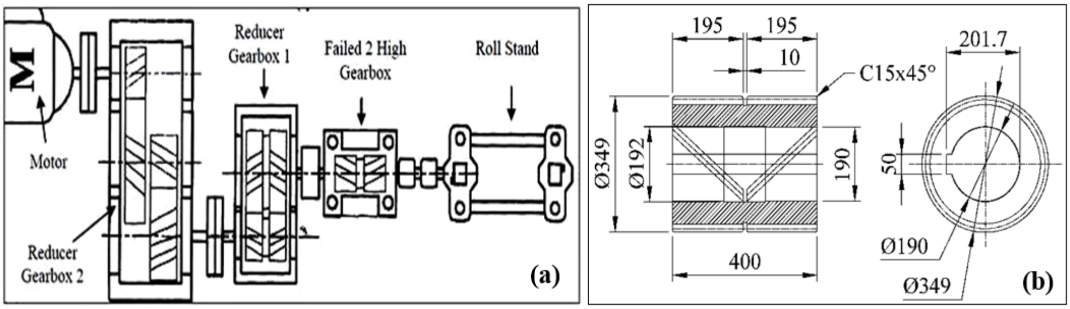


**Figure 1 Layout of the 2hi-PG with rolling stand (a) and key dimensions (mm) of the failed herringbone gear (b)**

## 3. Investigation Procedure

The failed gear was first inspected visually and macroscopically. Relevant dimensions were measured and details of operating conditions noted. Dye penetrant technique (DPT) was employed to enhance visual inspection of the crack and to reveal the nature of the crack more fully. Detailed measurements of dimensions of the key, keyway, shaft and bore of the failed gear were carried out to examine interference fits using a micrometer. Chemical analysis of the gear material was performed in order to identify the type of steel used. The chemical composition of the failed gear material was analysed using an optical emission spectrometer (Spectrolab Model Dv-4/202472-778A). Metallographic samples were prepared by cutting, grinding, polishing, and then etched using 2 % Nital. After etching, the microstructure of specimens was studied, and micrographs were taken using an optical microscope (LECO: IA32-Image analysis system). Fracture surface samples were ultrasonically cleaned in acetone. The samples were examined using a JEOL-JSM 5800 scanning electron microscope to examine the nature and details of the crack.

Stresses were calculated using the equations below and commercial finite element software. The finite element (FE) model was created in MSC Patran with MSC Nastran as the analysis tool. The bending stress on gear tooth during normal operation was calculated using equations 1-3 [12].

$$\sigma_b = W_t K_o K_v K_s \frac{1}{bm_t} \frac{K_H K_B}{Y_J} \tag{1}$$

$$W_t = \frac{2T}{D} \tag{2}$$

$$T = \frac{60{,}000 \times W_P}{2\pi n} \tag{3}$$

Where $\sigma_b$ is the bending stress (MPa), $W_p$ is electrical power (kW), $m_t$ is the module (mm), $b$ is a gear tooth face width (mm), $Y_J$ is a geometry factor for bending strength (including root fillet stress concentration factor), $K_o$ is the overload factor, $K_v$ is a velocity factor, $K_s$ is the size factor, $K_H$ is load distribution factor, $K_B$ is the rim-thickness factor, $W_t$ is tangential force on gear tooth (kN), $T$ is transmitted torque (Nm), $n$ is revolution of gear (rpm), and $D$ is pitch diameter (mm).

The FE model of the gear is simulated using 3D solid elements, HEX8, with an element global edge length of 5-10 mm. All of the solid elements are defined using Young's modulus value of 207 GPa and Poisson's ratio of 0.3. The geometry of the model reflects the actual dimensions of the gear. To simplify the FE model, the outer diameter of the model represents the diameter at the bottom of the gear teeth as shown in Figure 2a. Additional material of the gear teeth is considered to have only a small effect on the hoop stress in the gear.

There are 4 boundary conditions to constrain the model. (i) To simulate the deformation of the keyway due to the installation of the over-sized key, the nodes in the contact area are applied with a forced displacement of 0.5 mm, as shown in Figure 2b.

A contact area is the area which the keyway surface shows damages due to the interference as rubbing wear. (ii) To simulate an abutment between the bore of the gear and the shaft, the nodes at both sides of the bore are constrained in X translation because inside bore diameter of the gear cannot become smaller, as shown Figure 3a. (iii) To simulate another abutment contact between the shaft and the inside bore diameter of the gear, the nodes at the bottom of the inside bore diameter of the gear are constrained in Y translation, as shown in Figure 3b. (iv) There is one node which has been constrained in Y translation, this node is also constrained in all DOFs to locate the model in the space and to make the analysis runs.

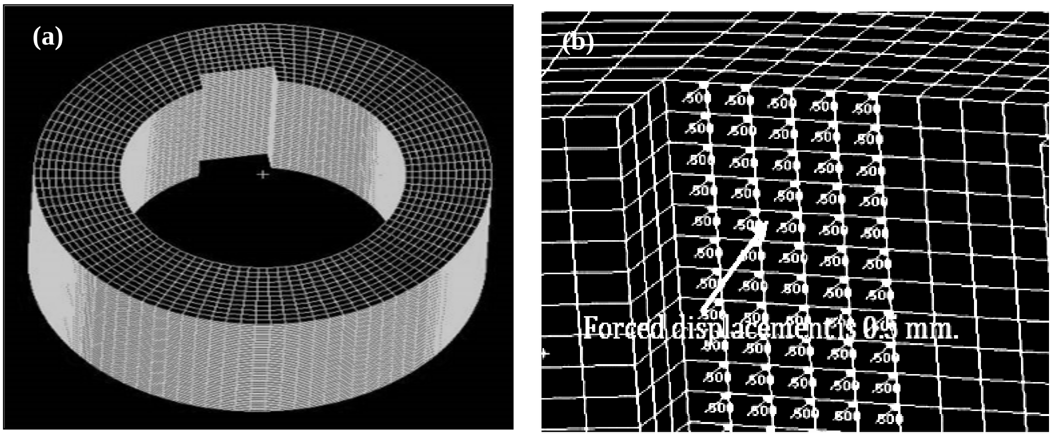


**Figure 2** Simplify the FE model of gear (a) Forced displacement on the keyway (b)

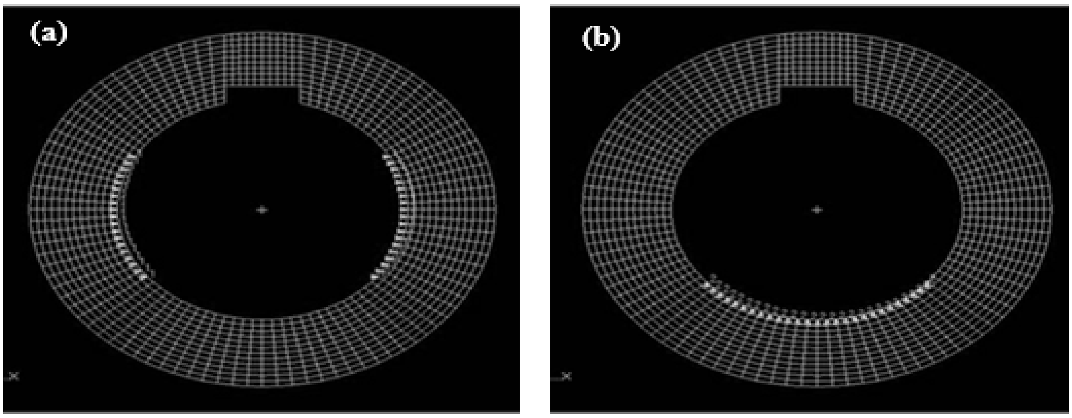


**Figure 3** Constrained in X translation (a) Constrained Y translation (b)

## 4. Results

### 4.1 Visual Examination

The appearances of the failed gear from various perspectives are shown in Figure 4. Figure 4a shown longitudinal crack on gear teeth, Figure 4b shown longitudinal crack running through approximate 370 mm (92%) of the gear face width (400 mm) and the initial crack occurred at root fillet of the gear teeth and toward to keyway seat as shown in Figure 4c.

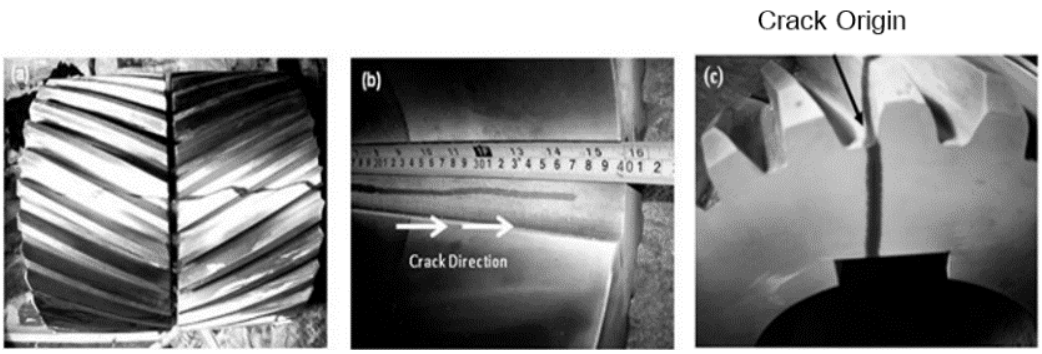


**Figure 4 Failed herringbone gear: (a) longitudinal crack, (b) direction of crack, and (c) crack origin**

The surface of keyway seat has interference fitting as heavy rubbing (black color) approximates 20 mm width of keyway and 300 mm long start from initial crack side as shown in Figure 5. It was indicated no clearance between the key and the keyway seat. Heavy rubbing on keyway seat was indicated using heavy force when assembly pressed the shaft into the bore of gear.

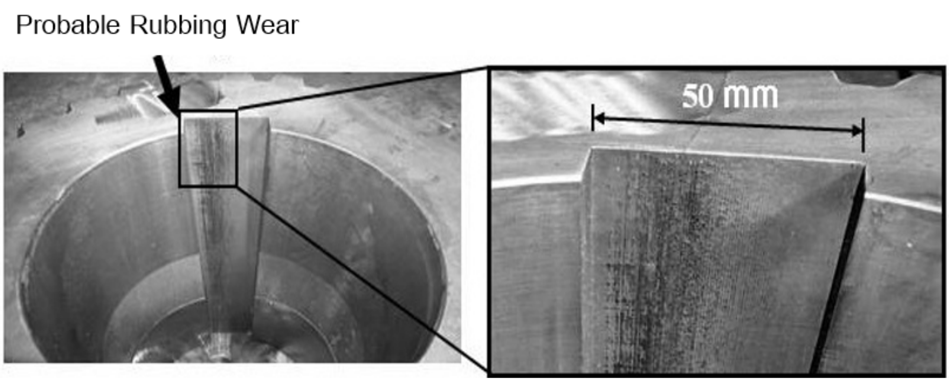


**Figure 5 The appearance of dark marks**

### 4.2 Detail Dimensional Examinations

The diameters of the shaft and the bore of the failed gear were 190.02 mm, 190.00 mm, respectively. The dimensions of the top keyway with shaft and the top keyway seat with bore of the failed gear were 200.20 mm and 201.70 mm respectively as shown in Figure 6. This means that the shaft with the key will be higher than the top keyway seat with the bore, and the interference is 0.50 mm.

It was indicated poor manufacturing due to assembly person no taking care of dimension of the key and the keyway to mount on a shaft. Normally, the top key should never be allowed to contact on the keyway seat. It is a good rule to allow from 0.50 to 0.76 mm clearance between the key and the bottom of the keyway seat.

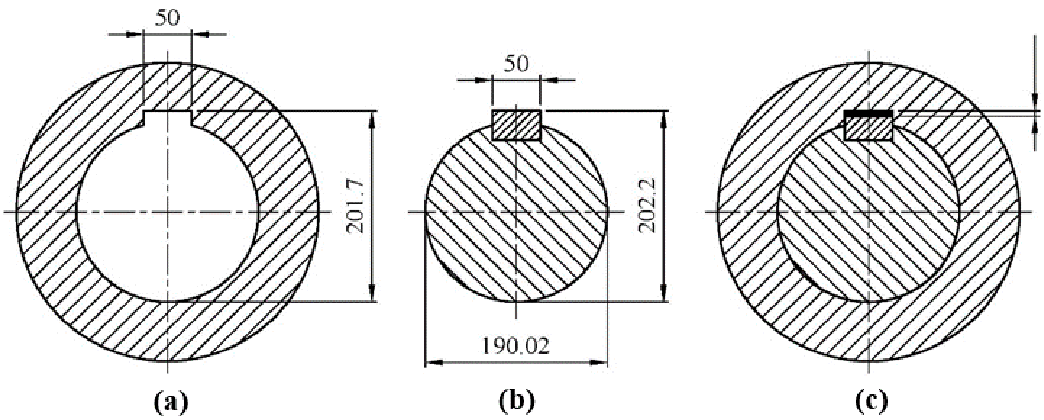


**Figure 6 The dimensions of the bore gear and the shaft (a) bore of the failed gear (b) the failed gear shaft and (c) interference**

### 4.3 Chemical Composition

The average values of the chemical compositions of the failed gear material are shown in Table 1. The compositions indicated that the gear material was made from low alloy Cr-Mo steel to JIS- SCM 440 standard [13]. The JIS-SCM 440 belongs to a class of high strength structural steel which are quenched and tempered hardenable. The SCM 440 steel is commonly and widely used in making gear [14].

**Table 1** **Chemical composition of the failed gear material and JIS-SCM 440 (%wt)**

| Material | Failed gear | JIS-SCM 440 |
|---|---|---|
| C | 0.392 | 0.38-0.45 |
| Si | 0.318 | 0.15-0.35 |
| Mn | 0.637 | 0.60-0.85 |
| S | 0.009 | 0.03 (max) |
| P | 0.022 | 0.03 (max) |
| Cr | 0.713 | 0.90-1.20 |
| Mo | 0.179 | 0.15-0.30 |

### 4.4 Fracture Morphology

The fracture surfaces reveal that the fracture surfaces are rock candy and dimples was observed at the fracture of the gear hub as shown in Figure 7. Additionally, the presence of extensive sub- surface cracks at the loading surface of the failed gear was an indication that during operation and keyway and key overlap. Crack occurred place between the grains and the fracture surface was intergranular fracture as shown in Figure 7. The fracture surface indicated that the gear was subjected to a very high stress mode 1. The fracture takes place between the grains; and that fracture surface has a "rock candy" appearance which reveals the shapes of the individual grain. The surface of the fracture tends to be perpendicular to the principal tensile stress.

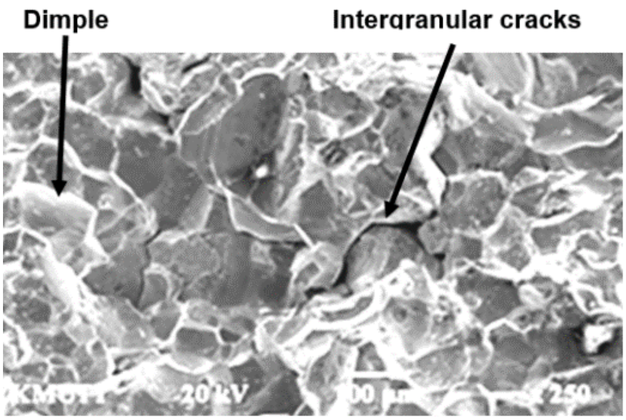


**Figure 7** **Fracture surface with intergranular cracks**

### 4.5 Microstructure Analysis

The case microstructure of the failed gear is homogeneous fine-laths tempered martensite as shown in Figure 8a. The core microstructure is tempered martensite as shown in Figure 8b. The microstructures of the case and core of the gear indicated that the failed gear material was quenched and tempered which is common practice in heat treatment of gears. No abnormality was found in the microstructure.

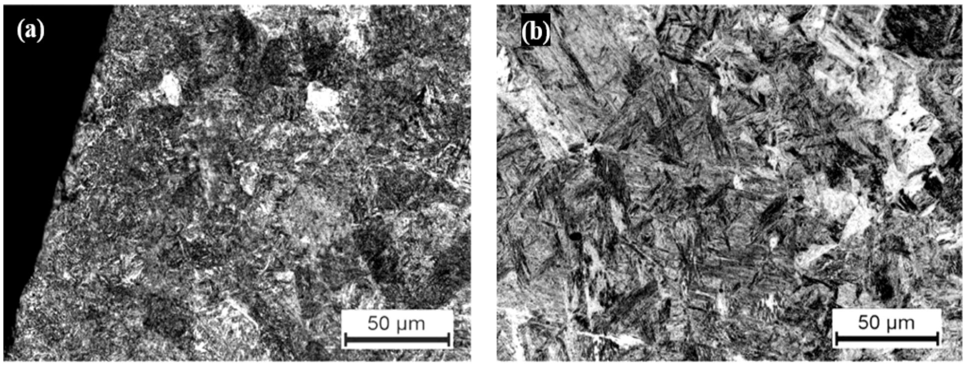


**Figure 8 The microstructure of gear material (a) homogeneous fine-laths of tempered martensite, (b) tempered martensite**

## 5. Stress Analysis

The values of various parameters used in calculating bending stress are shown in Table 2.

**Table 2 Parameters and values for calculating bending stress**

| Parameters | Symbol | Values | Unit |
|---|---|---|---|
| Electrical motor power | $W_p$ | 300 | kW |
| Pitch diameter of the gear | $D$ | 0.33 | m |
| Revolution of the gear | $n$ | 65.00 | rpm |
| Transmitted torque, T=$W_p$×60000/(2×¶×$n$) | $T$ | 44.00 | kNm |
| Module (equivalent from DP 2.25) | $m_t$ | 11.29 | mm |
| Tangential load | $W_t$ | 266.67 | kN |
| Width teeth | $b$ | 0.39 | M |
| Application or overload factor | $Ko$ | 1.75 | - |

**Table 2 Parameters and values for calculating bending stress (cont.)**

| Parameters | Symbol | Values | Unit |
|---|---|---|---|
| Velocity factor (Hobbed) | $K_v$ | 1.021 | - |
| Size factor | $K_s$ | 1.189 | - |
| Load distribution factor | $K_H$ | 1.65 | - |
| Rim-Thickness factor | $K_B$ | 1 | - |
| Geometry factor for bending | $Y_j$ | 0.38 | - |

Using equations 1-3 and the values in Table 2, the calculated bending stress ($\sigma_b$) on the loaded tooth during normal operating condition was 559 MPa.

Calculation by FE method, the result of the maximum principal stress at the outer surface due to key and keyway overlap was 545 MPa as shown Figure 9 which is from a combination of the overall hoop stress of the gear. The compressive stress of 904 MPa is at the surface of the keyway seat where the forced displacement is applied as shown in Figure 9, but the initial crack could not be started from the compressive side. It is initial crack start from the outside to keyway seat as it has the tensile stress. It can be seen that the stress due to the key and keyway overlap is as same the stress resulting from the load in normal operating condition.

The combined both stress (i.e. the bending stress from normal operation, that from key and keyway overlap) was 1104 MPa which were higher than material allowance leading initiated crack.

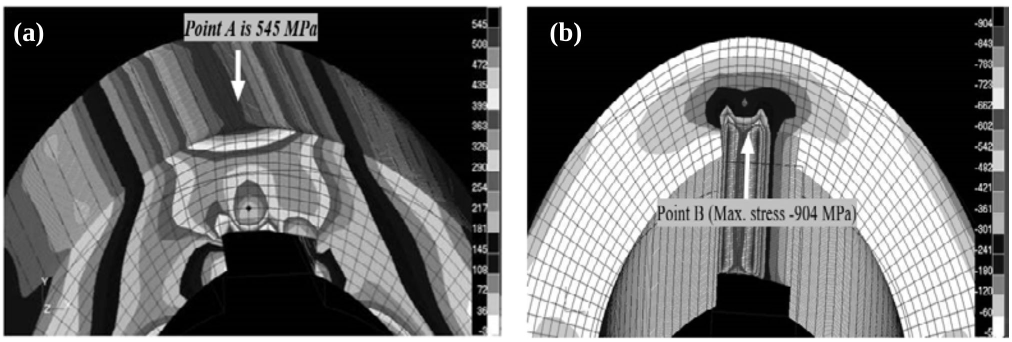


**Figure 9 Stress analysis (a) Maximum principal stress (tensile stress) (b) Maximum principal stress (compressive stress)**

## 6. Discussion

The keyway crack in question occurred at middle of keyway seat as shown in Figure 4c. Normally, the keyway cracking occurred at the corners of keyway which is high stress concentration [3]. Because the maximum principal stress from key and keyway overlap occurred at outer as shown at point A in Figure 9 and maximum bending stress due to normal operation condition with stress concentration occurred at same point where high stress is lead to initial crack from the root fillet gear tooth toward to middle of the keyway seat.

## 7. Conclusion and Recommendation

The cause of the herringbone gear failure was excessive stress resulting due to the keyway and the key overlaps lead to initial crack.

It is recommended the extreme care must be taken in main dimensional when using keys and keyways to assembly on a shaft the dimensions of the keyways and keys should be made in accordance with an accepted standard within the recommended value before assembly the herringbone gear into the shaft.

## Acknowledgement

The authors would like to thank Mr. Tawat Sopasit who is factory manager in the Jian-Ta steel Co., Ltd., Samutprakarn Thailand for his help in the history of the 2hi-PG and allowing the publication of this information.

## References

[1] Becker WT, Shipley RJ. ASM handbook volume 11: failure analysis and prevention. Metals park, OH: American society for metals; 1996.

[2] Failure atlas: adhesive wear-gear failure [Internet]. [cited 2017 Jan 15]. Available from https://onyxinsight.com/wind-turbine-failures-encyclopedia/gear-failures/adhesive-wear.

[3] Kohara gear industry Co., Ltd. Damage to gear [Internet]. 2015 [cited 2017 Dec 19]. Available from http://khkgears.net/gear-knowledge/gear-technical-reference/damage-to-gears/.

[4] Fernandes PJL. Tooth bending fatigue failures in gears. Eng Fail Anal 1996;3:219-25.

[5] Elecon engineering Co., Ltd. Power transmission & drive solution [Internet]. [cited 2017 Jul 20]. Available from http://www.elecon.com/gearworld/dat-dw-failure.html.

[6] Bruzek B, Leidich E. Investigation of influence of keyway on stress distribution in thin rimmed pinions. 22nd DANUBIA-ADRIA symposium on experimental method in solid mechanics; 2005 Sep 28-Oct 1; Parma, Italy. New York: Curran associates; 2005.

[7] Lewicki DG, Ballarini R. Effect of rim thickness on gear crack propagation path. Transactions of the ASME 1997;119:88-95.

[8] Peterson RE. Stress concentration factors. New York: John Wiley; 1974.

[9] Netpu S, Srichandr P. Failure analysis of a herringbone gear. Key Eng Mater 2011;462-463:366-71.

[10] Mancuso JR, Jones R. Coupling interface connection. Proceeding of the 30th Turbomachinery symposium 2002. Texas: Texas A&M University; 2002. p.121-38.

[11] Principles of bearing selection and applications. SKF General catalogue. Germany: 2003.

[12] Norton RL. Machine design: An integrated approach. 3rd ed. New York: Prentice hall; 2006.

[13] JIS handbook - Ferrous materials & metallurgy I. Tokyo: Japan standards association; 2002.

[14] Bangkok special steel Co., Ltd. Machinery steel [Internet]. [cited 2017 April 20]. Available from http://www.bssteel.co.th/product_en.html.

**Author's Profile**

**Somdech Ingkawara** received the B.E. (1992) in degree Industrial Engineering from Rajamangala University of Technology Lanna, M.PE. (1999) in Production Engineering from King Mongkut's University of Technology North Bangkok. He is a lecturer, Department of Industrial Engineering, Faculty of Engineering, Pathumwan Institute of Technology. Research field: Machining, Manufacturing Processes, Failure Analysis,

**Samroeng Netpu, D. Eng**. Lecturer of Master of Engineering in Engineering Management Program. He has graduated in Bachelor of Engineering in Mechanical Engineering at King Mongkut's University of Technology Thonburi, Master of Engineering in Engineering Management at Kasem Bundit University and Doctor of Engineering in Integrated Product Design and Manufacturing at King Mongkut's University of Technology Thonburi.

**Article History:**

Received: December 12, 2018

Revised: February 18, 2019

Accepted: March 7, 2019